Molecular Crystals and Liquid Crystals

Publication details, including instructions for authors and subscription information:
http://www.tandfonline.com/loi/gmcl20

Contribution of Electrostatic Energy to Curvature and Frank Elastic Energy of Monolayer Domains Comprised of Polar Molecules: Shape of Domains with Orientational Deformation

Tetsuya Yamamoto [a b], Takaaki Manaka [c] & Mitsumasa Iwamoto [c]

[a] Department of Physical Electronics, Tokyo Institute of Technology, Meguro-ku, Tokyo, Japan

[b] JSPS-fellow, Chiyoda-ku, Tokyo, Japan

[c] Department of Physical Electronics, Tokyo Institute of Technology, Meguro-ku, Tokyo, Japan

Version of record first published: 22 Sep 2010

To cite this article: Tetsuya Yamamoto, Takaaki Manaka & Mitsumasa Iwamoto (2007): Contribution of Electrostatic Energy to Curvature and Frank Elastic Energy of Monolayer Domains Comprised of Polar Molecules: Shape of Domains with Orientational Deformation, Molecular Crystals and Liquid Crystals, 479:1, 33/[1071]-47/[1085]

To link to this article: http://dx.doi.org/10.1080/15421400701732464

Mol. Cryst. Liq. Cryst., Vol. 479, pp. 33/[1071]–47/[1085], 2007

ISSN: 1542-1406 print/1563-5287 online
DOI: 10.1080/15421400701732464

Contribution of Electrostatic Energy to Curvature and Frank Elastic Energy of Monolayer Domains Comprised of Polar Molecules: Shape of Domains with Orientational Deformation

Tetsuya Yamamoto
Department of Physical Electronics, Tokyo Institute of Technology, Meguro-ku, Tokyo, Japan; JSPS-fellow, Chiyoda-ku, Tokyo, Japan

Takaaki Manaka
Mitsumasa Iwamoto
Department of Physical Electronics, Tokyo Institute of Technology, Meguro-ku, Tokyo, Japan

The domain shape formation of monolayers comprised of polar molecules with the orientational deformation of spontaneous polarization is investigated by viewing this problem as electrostatic charge effect. The orientational deformation contributes to the domain free energy as the spontaneous curvature, Frank elastic energy, and spontaneous splay, which originate from the effect of diagonal and off-diagonal components of capacitance matrix. Shape equation is extended by introducing the concept of "curvature of polarization" to take into account the spontaneous curvature. It is exemplified that the spontaneous curvature is reasonably understood as the shape formation to optimize the off-diagonal component of electrostatic energy.

Keywords: electrostatic charge effect; monolayer domain shapes; shape equation; spontaneous curvature

PACS Numbers: 68.18.-g; 61.30.DK

The authors thank Prof. Z. C. Ou-Yang (The Chinese Academy of Science) for fruitful discussion. This work was supported by the Grants-in-Aid for Scientific Research of JSPS.

Address correspondence to Mitsumasa Iwamoto, Department of Physical Electronics, Tokyo Institute of Technology, 2-12-1 S3-33 O-okayama, Meguro-ku, Tokyo 152-8552, Japan. E-mail: iwamoto@ome.pe.titech.ac.jp

I. INTRODUCTION

Physicochemical properties of amphiphile monolayers at the air-water interface have attracted much attention since the preparation technique was developed by Langmuir [1,2]. The structure of monolayers is determined by the positional order of molecular head on the water surface and orientational order of molecular tail pointing toward the air. The orientational order parameters $S_n(=\langle P_n(\cos\theta)\rangle)$ are introduced as an extension of orientational order parameter S_2 of nematic liquid crystal [3], where $P_n(\cos\theta)$ is the Legendre polynomial of nth rank ($n = 1, 2, \ldots$) and θ is the tilt angle of molecular long axis from the director. The non-centrosymmetric structure of monolayers is characterized by the presence of odd-number-th rank orientational order parameters, i.e., $S_{2m-1} \neq 0$ ($m = 1, 2, \ldots$). From the viewpoint of dielectric physics of monolayers, the spontaneous and second order non-linear polarizations are generated from monolayers since monolayers possess non-zero S_1 and S_3 ($S_1 \neq 0$ and $S_3 \neq 0$) [4]. In other words, the electrostatic energy is stored in monolayers due to the generation of the spontaneous polarization. We have developed Maxwell displacement current (MDC) and optical second harmonic generation (SHG) measurement techniques to detect the spontaneous and non-linear polarizations, and have measured the S_1 and S_3 of monolayers comprised of rod-shaped molecules, e.g. alkyl-cyanobiphenyl homologues [5]. The liquid crystal-like properties, e.g. flow reorientation [6,7] and flexoelectric effect [8], of monolayers are also detected by MDC-SHG measurements, and the nematic order parameter S_2 was measured from monolayers in condensed phase by Brewster angle reflectometry (BAR) [9,10]. However, this approach is still not sufficient to characterize the physicochemical properties of monolayers in two-phase coexistent state due to the presence of domain structure of monolayers.

A variety of characteristic shapes of monolayer domains have been observed by Brewster angle microscopy (BAM) [11–14] and fluorescent microscopy [15,17,23]. In the determination of shapes of 3D materials ($S_1 = 0$), the surface tension often makes a dominant contribution. On the other hand, since monolayers possess non-zero S_1, the electrostatic energy is stored in monolayer domains due to the dipole-dipole interaction, and plays an important role in the formation of domain shapes of monolayers. It naturally links to McConnell's model [16] that the domain shapes of monolayers are determined by the competition between the dipole-dipole interaction and line tension λ (2D analogue of surface tension), i.e. the free energy of monolayer domain is written as [16]

$$F = \lambda_0 \oint ds + F_\perp + F_\parallel, \tag{1}$$

where $F_\perp$ and $F_\parallel$ are the contribution of water surface normal and in-plane components of dipole moment density, respectively. Though the McConnell's model has been supported by some experimental evidences [17], it was only applied to a few predetermined shapes, e.g. circle [16,17], owing to the mathematical difficulty in calculating $F_\perp$ and $F_\parallel$. In order to overcome this difficulty, the McConnell's model has been reformulated from the viewpoint of differential geometry in our previous studies [18,19]. Using Taylor expansion method, $F_\perp$ is approximately expressed in terms of the curvature κ and boundary length L (see Eq. (5)) in the similar form to the Helfrich's shape free energy of lipid vesicle [20]. Mapping $F_\perp$ to the shape free energy of lipid vesicles, the shape equation of monolayer domains with $F_\parallel = 0$ was derived on the analogy of the shape equation of lipid vesicle as [18]

$$\Delta P - \lambda_\perp \kappa + \alpha_\perp \kappa^3 + 2\alpha_\perp \kappa_{ss} = 0, \tag{2}$$

where $\lambda_\perp = \lambda_0 - \mu_\perp/2\ln(eL/h) + 11/48 L\mu_\perp^2 \oint \kappa^2 ds$ and $\alpha_\perp = 11/96\,\mu_\perp^2 L^2$. κ is a function of boundary length s. $\mu_\perp$ is the normal component of dipole density. In this theory, we additionally introduced $\Delta P(=\Pi - g_0)$ to take into account the contribution of surface pressure Π and the Gibbs energy density difference g_0 between outer phase and inner phase. The contribution of $F_\parallel$ to the formation of domain shapes is also studied through the approach of differential geometry. $F_\parallel$ of domains with uniform in-plane polarization is represented approximately as curvature elastic energy (see Eq. (6)), where elastic constant is dependent on the angle between tilt direction and boundary normal $\psi(\kappa = -d\psi/ds)$. The shape equation of monolayer domains with uniform in-plane dipole density $\mu_\parallel$ is derived as [19]

$$\begin{aligned}\Delta P - \lambda_\parallel \kappa + \alpha_\parallel \kappa^3 + 2\alpha_\parallel \kappa_{ss} + 3\tau\kappa\cos 2\psi + 2\zeta\kappa_{ss}\cos 2\psi \\ - 3\zeta k^3 \cos 2\psi + 8\zeta\kappa\kappa_s \sin 2\psi = 0,\end{aligned} \tag{3}$$

where $\zeta = 13/192\mu_\parallel^2 L^2$, $\tau = 1/4\,\mu_\parallel^2 \ln(L/h)$, $\alpha_\parallel = \alpha_\perp - 11/192\mu_\parallel^2 L^2$, $\lambda_\parallel = \lambda_\perp + \tau + 1/(2L)\mu_\parallel^2 \int \cos^2\psi ds + 2/L \int(-11/192\mu_\parallel^2 L^2 + \zeta\cos 2\psi)\kappa^2 ds$. Equation (3) returns to Eq. (2) when $\mu_\parallel = 0$. The growth of clover shaped domains from circular domains, which is observed from racemic DPPC monolayers [15], has been predicted on the basis of Eq. (3) [19].

Domains with orientational deformation have also been observed by BAM and polarized fluorescent microscopy (PFM) from e.g. fatty acid monolayers [13] and chiral DPPC monolayers [14]. It indicates the importance of orientational deformation, i.e. liquid crystal-like properties of monolayers, in the formation of domain shapes of such monolayers. Rudnick and Bruinsma have phenomenologically introduced the free energy comprised of Frank elastic energy and anisotropic line tension on the analogy of elastic theory of liquid crystal [21], and have

reproduced the cusped shape of fatty acid monolayer domains [13]. However, it is indispensable to clarify this problem from the electrostatic viewpoint for the clear and unified physical picture of domain shape formation. Recently, we have analyzed the contribution of orientational deformation to the formation of domain shapes by viewing it as the electrostatic charge effect [22]. The dipole moment density ($\mu_\perp$ and $\mu_\parallel$) is actually equivalent to the spontaneous polarization ($\mathbf{P}_0(\mathbf{R})$) in dielectric physics. The electrostatic energy of a domain due to the generation of spontaneous polarization is rewritten as the interaction between induced charge at the internal part and boundary of a domain. Using Taylor expansion, the electrostatic energy is approximately expressed as the Frank elastic energy with spontaneous splay and curvature energy with spontaneous curvature, where they are ascribed to the effect of diagonal and off-diagonal components of capacitance matrix. The derived free energy is analogous to the free energy introduced phenomenologically by Rudnick and Bruinsma. The values used to reproduce cusped shape of fatty acid domains are validated on the ground of this approach [25]. In the present study, we analyze the contribution of orientational deformation of spontaneous polarization to the formation of domain shapes from the viewpoint of differential geometry for the further understanding of forming mechanism of domain shapes. As a first step, we focus on the contribution of the spontaneous curvature in this article. We introduce the "curvature of polarization" χ to represent the orientational deformation, and derive a shape equation taking into account the effect of spontaneous curvature as an extension of Eq. (3). In order to clealy show the effect of χ, we carry out a model calculation for domains with simple bend orientational deformation. We found that egg-like domain shapes, where similar shapes have been observed from DMPA monolayers [23], are a solution of the shape equation (see Fig. 4). It is exemplified that the spontaneous curvature is reasonably understood as shape formation to optimize the off-diagonal components of capacitance matrix.

II. SHAPE FREE ENERGY OF MONOLAYER DOMAINS WITH ORIENTATIONAL DEFORMATION

Here, we briefly summarize our approach to the domain shape formation by viewing it as electrostatic charge effect [22]. In electrostatic theory, charges are induced by splay orientational deformation of spontaneous polarization ($\rho_{induced} = -\nabla \cdot \mathbf{P}_0(\mathbf{R})$). Thus, the electrostatic energy ($F_e = F_\perp + F_\parallel$) due to the generation of spontaneous polarization $\mathbf{P}_0(\mathbf{R})$ is written as [22]

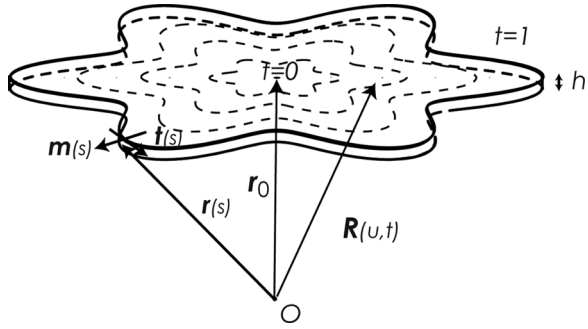

FIGURE 1 Geometry of monolayer domain. $\mathbf{r}(s)$, $\mathbf{t}(s)$, and $\mathbf{m}(s)$ are the positional vector of domain boundary, tangent vector, and normal vector, respectively, and are functions of length s. When we fill the internal part of domains with the domain boundary curve with different scale t ($0 \le t \le 1$), positions in the internal part are represented by u ($=ts$), ($0 \le u \le L$) and t as $\mathbf{R}(u, t)$.

$$
\begin{aligned}
F_e = &-\frac{P_{0\perp}^2}{2}\int ds_i \int ds_j \frac{\mathbf{t}(s_i)\cdot\mathbf{t}(s_j)}{|\mathbf{r}(s_i)-\mathbf{r}(s_j)|} \\
&+\frac{1}{2}\int ds_i \int ds_j \frac{\mathbf{P}_0(\mathbf{r}(s_i))\cdot\mathbf{m}(s_i)\mathbf{P}_0(\mathbf{r}(s_j))\cdot\mathbf{m}(s_j)}{|\mathbf{r}(s_i)-\mathbf{r}(s_j)|} \\
&-\frac{1}{2}\int ds_i \int dS_j \frac{\nabla_j\cdot\mathbf{P}_0(\mathbf{R}_j)\mathbf{P}_0(\mathbf{r}(s_i))\cdot\mathbf{m}(s_i)}{|\mathbf{r}(s_i)-\mathbf{R}_j|} \\
&-\frac{1}{2}\int dS_i \int ds_j \frac{\nabla_i\cdot\mathbf{P}_0(\mathbf{R}_i)\mathbf{P}_0(\mathbf{r}(s_j))\cdot\mathbf{m}(s_j)}{|\mathbf{R}_i-\mathbf{r}(s_j)|} \\
&+\frac{1}{2}\int dS_i \int dS_j \frac{\nabla_j\cdot\mathbf{P}_0(\mathbf{R}_i)\nabla_j\cdot\mathbf{P}_0(\mathbf{R}_j)}{|\mathbf{R}_i-\mathbf{R}_j|},
\end{aligned}
\tag{4}
$$

where $\mathbf{r}(s)$, $\mathbf{t}(s)$, and $\mathbf{m}(s)$ are the positional vector, tangent vector, and normal vector of domain boundary, respectively, and are functions of arc-length s (see Fig. 1). $|\mathbf{R}_i - \mathbf{R}_j|$ is the distance between the two different positions $\mathbf{R}_i$ and $\mathbf{R}_j$ in the internal area of a domain. $\mathbf{R}_i$ and $\mathbf{R}_j$ are 2D positional vectors (see Fig. 1). dS is the area elements. ∇ is 2D gradient operator. $P_{0\perp}$ represents the water surface normal component of the spontaneous polarization. The first and second terms are the contribution of $F_\perp$ and the interaction between charges induced at the domain boundary ($\sigma_{induced} = \mathbf{P}_0(\mathbf{r}(s))\cdot\mathbf{m}(s)$), respectively, and are partly taken into account in Eq. (3) [18,19]. The third and fourth terms are the interaction between charges $\rho_{induced}$ induced at the internal part and charges $\sigma_{induced}$ induced at the domain boundary. The fifth term is the interaction between charges $\rho_{induced}$ induced at the

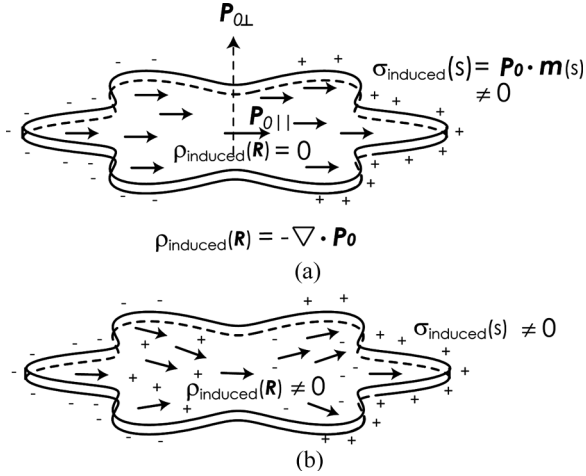

FIGURE 2 (a) Monolayer domain with uniform tilt of spontaneous polarization. Charge density is only at the boundary. (b) Monolayer domain with tilt orientational deformation of spontaneous polarization. Charge density is induced at the internal part and boundary of domain.

internal part. When the spontaneous polarization is generated uniformly in a domain ($\nabla \cdot \mathbf{P}_0 = 0$), only the first and second terms are non-zero (Fig. 2(a)). On the other hand, when the spontaneous polarization forms orientational deformation in a domain ($\nabla \cdot \mathbf{P}_0 \neq 0$), all terms of Eq. (4) are non-zero (Fig. 2(b)).

Taylor expansion method is useful to clearly express the contribution of electrostatic energy to the formation of domain shapes [18,19]. In the following, we expand each term of Eq. (4) using this method. The first term of Eq. (4) is approximately calculated as

$$F_\perp = -\frac{P_{0\perp}^2}{2}\ln\frac{L}{h}\oint ds + \frac{11}{96}P_{0\perp}^2 L^2 \oint \kappa^2 ds, \tag{5}$$

i.e., the sum of the negative line tension and elastic energy in terms of κ (see Eq. (7) in ref. [18]). In the same way, the second term of Eq. (4) is rewritten as

$$F_{2nd} = \int ds \lambda_{2nd}(s) + \int ds[\alpha_\parallel(s)(\kappa^2 - 2\kappa_0\kappa)], \tag{6}$$

where $\alpha_\parallel(s) = L^2/96\ \sigma_{induced}^2 - L^2/8\ [\mathbf{P}_0(\mathbf{r}(s)) \cdot \mathbf{t}(s)]^2$, $\lambda_{2nd}(s) = 1/2\ln(L/h)\sigma_{induced}^2 - L^2/8[(d\mathbf{P}_0(\mathbf{r}(s))/ds) \cdot \mathbf{m}(s)]$, and $2\alpha_\parallel(s)\kappa_0 = L^2/4[\mathbf{P}_0(\mathbf{r}(s)) \cdot \mathbf{t}(s)][(d\mathbf{P}_0(\mathbf{r}(s))/ds) \cdot \mathbf{m}(s)]$. Equation (6) returns to the

equation used in Ref. [19] when $\mathbf{P}_0$ is uniform. $\lambda_{2nd}(s)$ and $\alpha_{\|}(s)$ are anisotropic line tension and elastic energy. κ_0 is the spontaneous curvature. Note that $\kappa_0 = 0$ when the spontaneous polarization is uniform. Equation (6) is further rewritten as

$$F_{2nd} = \frac{1}{2}\ln\frac{L}{h}\int ds\sigma_{induced}(s)^2 + \frac{L^2}{96}\int ds\kappa^2\sigma_{induced}(s)^2 - \frac{L^2}{8}\int ds\left(\frac{d}{ds}\sigma_{induced}(s)\right)^2. \quad (7)$$

The first and second terms represent the contributions of diagonal components of capcitance matrix, and third term represents the contribution of off-diagonal components of capacitance matrix. $d\sigma_{induced}(s)/ds$ is written as the sum of the charge density induced by the curvature of a domain shape $-\kappa\mathbf{P}_0(\mathbf{r}(s))\cdot\mathbf{t}(s)$ and that induced by orientational deformation $(d\mathbf{P}_0(\mathbf{r}(s))/ds)\cdot\mathbf{m}(s)$. The spontaneous curvature originates from the interaction between the charge density induced by curvature κ and the charge density induced by orientational deformation. κ_0 is the curvature of the shape, which minimizes the second term of Eq. (6), due to the presence of charge density induced by the orientational deformation. In sec. III, we discuss the contribution of κ_0 to the formation of domain shapes in detail.

In order to apply Taylor expansion on the third, fourth, and fifth terms of Eq. (4), let us express positions $\mathbf{R}$ in the internal part of a domain by u $(\equiv s/t)$ and t $(0 \le t \le 1)$ as (see Fig. 1) $\mathbf{R}(u,\ t) = t\mathbf{r}(u) - t/L\oint ds'\mathbf{r}(s') + \mathbf{r}_0$, where $\mathbf{r}_0$ is the center of gravity of a domain shape $(t = 0)$ and $\boldsymbol{R}(u,1) = \mathbf{r}(s) - 1/L\oint ds'\mathbf{r}(s')$ $(t = 1)$. This coordinate represents the positions at the internal part of a domain by scale t and length ut of scaled boundary curve with the identical center of gravity. The extension of Taylor expansion method to 2D is described in ref. [22]. When the gradient of $\nabla\cdot\mathbf{P}_0$ is not steep, the fifth term of Eq. (4) is written as [22]

$$F_{5th} \sim \frac{1}{2}L\int dSK_{11}(u,t)(\nabla\cdot\mathbf{P}_0)^2, \quad (8)$$

where $LK_{11}(u,\ t) = \int_0^L dx\int_0^L dy[\sqrt{g(u,\ t)}/|\mathbf{R}(u,\ y) - \mathbf{R}(u\ +\ x,\ t)|] - \partial/\partial u(\int_0^L dx\int_0^1 dy\sqrt{g(u,y)}x|\mathbf{R}(u,y) - \mathbf{R}(u+x,t)|) + 1/2\partial^2/\partial u^2(\int_0^L dx\int_0^L dy[\sqrt{g(u,y)}x^2/|\mathbf{R}(u,y) - \mathbf{R}(u+x,t)|])$. $dS = \sqrt{g(u,t)}dudt$ is the area element [20]. Equation (8) indicates that the contribution of fifth term of Eq. (4) is the Frank elastic energy [3] in terms of splay deformation of spontaneous polarization, where elastic coefficient is a function of position and shape. Equation (8) is nothing but the electrostatic

energy ascribed to the storage of charge density ρ_{induced} at capacitance density $C^{-1}(u,t) = LK_{11}(u,t)$, where $C^{-1}(u,t)$ is the voltage required to store unit charge density at (u,t). C^{-1} of the center of uniformly charged circular domain is L. Thus, $K_{11}(u, t)$ is the geometrical factor, which represents the deviation of C^{-1} from the center of circular domain due to the deviation of position and domain shape. Similarly, the sum of third and fourth terms of Eq. (4) are expanded as

$$F_{3rd} + F_{4th} = -\int dsK_1(u,t)\nabla \cdot \mathbf{P}_0(u,t), \tag{9}$$

where $K_1(u,t) = \int_0^L dx(\mathbf{P}_0(\mathbf{r}(u+x)) \cdot \mathbf{m}(u+x))/|\mathbf{r}(u+x,1) - \mathbf{r}(u,t)|$. Thus, the third and fourth terms of Eq. (4) contribute as spontaneous splay to the formation of domain shapes. $K_1(u, t)$ is dependent on the charge $\sigma_{induced} (= \mathbf{P}_0 \cdot \mathbf{m}(s))$ at the domain boundary. When there are induced charges at the domain boundary ($K_1(u,t) \neq 0$), charges of opposite polarity are induced at the internal part of the domain to converge the force field from the boundary charge, and to maintain the charge neutrality of a domain. The splay orientational deformation is formed to induce such charges at the internal part. This effect is an origin of spontaneous splay deformation of monolayer domain.

III. CONTRIBUTION OF SPONTANEOUS CURVATURE TO MONOLAYER DOMAIN SHAPES WITH ORIENTATIONAL DEFORMATION

We consider a small variation ($\eta \ll 1$) of domain shape $\mathbf{r}'(s') = \mathbf{r}(s) + \eta(s)\mathbf{m}(s)$. Shape equation is derived as a stability condition

$$\delta F = \Delta P \delta \int dS + \lambda_0 \delta \oint ds + \delta F_e = 0, \tag{10}$$

where it represents a balance of force applied at the domain boundary [18–20]. The shape equation is derived by the direct substitution of Eqs. (5), (6), (8), and (9) into Eq. (10). However, the shape equation derived by the direct calculation is very complex, and does not provide clear physical picture on the effect of orientational deformation of spontaneous polarization on domain shapes. The spontaneous curvature κ_0 makes the most significant contribution to the formation of domain shapes among the contribution of orientational deformation of $\mathbf{P}_0$ since the spontaneous curvature originates from the interaction between induced charges at the boundary. As a first step, we focus on the contribution of the spontaneous curvature κ_0 to the formation of domain shapes in this article. According to Helmoholtz's theorem, vector fields, e.g. the spontaneous polarization $\mathbf{P}_0$, are written as the

sum of solenoidal component $\mathbf{V}_{sol}(\nabla \cdot \mathbf{V}_{sol} = 0$ and $\nabla \times \mathbf{V}_{sol} \neq 0)$ and irrotational component $\mathbf{V}_{irr}(\nabla \cdot \mathbf{V}_{irr} \neq 0$ and $\nabla \times \mathbf{V}_{irr} = 0)$. The solenoidal component does not contribute to Eqs. (8) and (9), but only contributes to the spontaneous curvature κ_0. In other words, our present framework is sufficient to investigate the shapes of domains with solenoidal orientational deformation of spontaneous polarization. In the following, we mainly analyze the shapes of domains with solenoidal orientational deformation to continue our discussion in the context of observed domain shapes. In order to investigate the shapes of domain with irrotational orientational deformation, we need to clarify the contribution of Eqs. (8) and (9). This is, however, our future work [25]. On the analogy of the physics of liquid crystal, we assume that the magnitude $P_{0\|}$ of in-plane component of spontaneous polarization is uniform, and that only the direction of spontaneous polarization possesses spatial gradient. Then, we introduce "curvature of polarization" χ_x and χ_y as

$$\begin{aligned} \frac{\partial}{\partial x}\mathbf{a}_{\|} &= \chi_x \mathbf{a}_{\perp} \\ \frac{\partial}{\partial x}\mathbf{a}_{\|} &= \chi_y \mathbf{a}_{\perp} \end{aligned} \tag{11}$$

to represent orientational deformation, where x and y are two orthogonal direction in the monolayer plane, and $\mathbf{a}_{\|}$ and $\mathbf{a}_{\perp}$ are in-plane unit vectors parallel and perpendicular to the orientation of in-plane component of spontaneous polarization, respectively. χ_x and χ_y are derivatives of the angle $\phi(x,y)$ of $\mathbf{a}_{\|}$ measured from a certain in-plane reference direction $((\chi_x, \chi_y) = \nabla\phi(x,y))$.

Shape equation of monolayer domains with uniform tilting of spontaneous polarization, i.e., $\mathbf{a}_{\|}$ is a constant vector, is derived as Eq. (3) [19]. Here, we discuss the shape equation of monolayers with spontaneous curvature extending Eq. (3). In the similar manner to ref. [19], we express $\mathbf{m}$(s) and $\mathbf{t}$(s) as

$$\mathbf{m}(s) = \cos\psi\mathbf{a}_{\|} + \sin\psi\mathbf{a}_{\perp} \tag{12}$$

$$\mathbf{t}(s) = -\sin\psi\mathbf{a}_{\|} + \cos\psi\mathbf{a}_{\perp}, \tag{13}$$

where $\psi(s)$ is the angle between the in-plane component of spontaneous polarization $\mathbf{a}_{\|}$ and boundary normal $\mathbf{m}(s)$. When $\mathbf{a}_{\|}$ is a constant vector, a relationship $\kappa = -\psi_s$ is satisfied on the basis of Frenet-Seret theorem [20]. This relationship plays a key role to derive Eq. (3) [19]. In the differential geometry, $-\kappa\Delta s$ is the angle between $\mathbf{m}(s+\Delta s)$ and $\mathbf{m}(s)$ (see Fig. 3). When $\mathbf{a}_{\|}$ is fixed, $\psi(s+\Delta s) - \psi(s) = -\kappa\Delta s$ $(\psi_s = -\kappa)$. On the other hand, when domains possess orientational deformation of

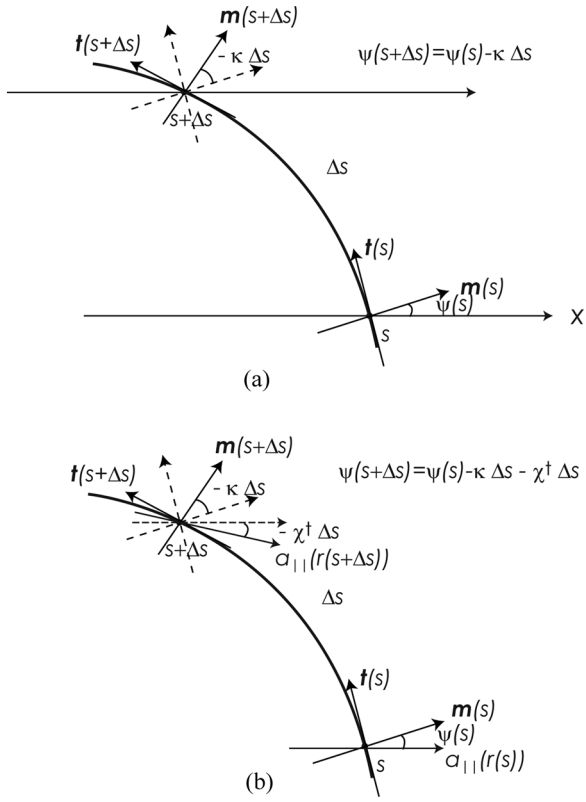

FIGURE 3 A geometrical meaning of curvature and curvature of polarization. ψ is the angle between the in-plane component of spontaneous polarization and boundary normal. (a) the contribution of curvature to the derivative of ψ ($\psi_s = -\kappa$). (b) the contribution of curvature and curvature of polarization to the derivative of ψ ($\psi_s = -\kappa - \chi^t$).

spontaneous polarization, $\mathbf{a}_{||}$ is no longer fixed, and $\mathbf{m}$ as well as $\mathbf{a}_{||}$ change along the domain boundaries (Fig. 3(b)). The curvature of polarization along the domain boundary is written as

$$\frac{d}{ds}\mathbf{a}_{||}(\mathbf{r}(s)) = \chi^t \mathbf{a}_{\perp}(\mathbf{r}(s)), \tag{14}$$

where $\chi^t = \mathbf{t}(s) \cdot \nabla\phi(\mathbf{r}(s))$. Substituting Eqs. (12) and (13) into Frenet-Seret theorem, we obtain

$$\psi_s = -\kappa - \chi^t. \tag{15}$$

The angle between $\mathbf{m}(s+\Delta s)$ and $\mathbf{m}(s)$ and angle between $\mathbf{a}_{\|}(\mathbf{r}(s+\Delta s))$ and $\mathbf{a}_{\|}(\mathbf{r}(s))$ are $-\kappa\Delta s$ and $-\chi^t\Delta s$, respectively (see Fig. 3). Hence, the total derivative of ψ along the domain boundary due to the change of $\mathbf{m}$ and $\mathbf{a}_{\|}$ is represented by Eq. (15). The charge density induced at the domain boundary is $\sigma_i = P_{0\|}\cos\psi$, and is dependent on χ^t as well as κ. Thus, the domain shapes, which optimize Eq. (6), are determined by the curvature of polarization χ^t. This effect is nothing but the spontaneous curvature κ_0 (see Eq. (6)). Actually, κ_0 is proportional to χ^t ($2\alpha_{\|}(s)\kappa_0 = -(L^4/4)P_{0\|}^2\chi^t\sin^2\psi$). Equation (10) is expressed in terms of the curvature of polarization χ^t and $\chi^m(=\mathbf{m}(s)\cdot\Delta\phi(\mathbf{r}(s)))$. Provided that curvature of polarizations, χ^t and χ^m, are so small that only linear terms of χ^t and χ^m are important, the shape equation of monolayer domains with orientational deformation of spontaneous polarization is represented as

$$\begin{aligned}\Delta P &- \lambda_{\|}\kappa + \alpha_{\|}\kappa^3 + 2\alpha_{\|}\kappa_{ss} + 3\tau\kappa\cos 2\psi + 2\zeta\kappa_{ss}\cos 2\psi - 3\zeta\kappa^3\cos 2\psi \\ &+ 8\zeta\kappa\kappa_s\sin 2\psi + 4\tau\chi^t\cos 2\psi + 2\tau\chi^m\sin 2\psi + 8\zeta\chi^t\kappa_s\sin 2\psi \\ &- 12\zeta\chi^t\kappa^2\cos 2\psi + 6\zeta\chi^m\kappa^2\sin 2\psi = 0. \qquad (16)\end{aligned}$$

This equation returns to Eq. (3) when $\chi^t = 0$ and $\chi^m = 0$. Note that $\lambda_{\|}$, $\alpha_{\|}$, τ, and ζ are the same values as those used in Eq. (3). Thus, there is no need to introduce extra effective elastic constants in our present theory. The effect of spontaneous curvature is represented by the last five terms (the ninth-thirteenth terms).

In order to investigate the contribution of spontaneous curvature more clearly, we carry out a model calculation of Eq. (16). In our previous study [19], we found that the circular domains with radius a such that $\tau^\circ = \zeta^\circ a^{-2}$ is a solution when $\chi^t = 0$ and $\chi^m = 0$, where the suffix $^\circ$ represents the circular domain. Such domains are formed at the surface pressure $\Delta P = -\lambda_{\|}^\circ + \alpha_{\|}^\circ a^{-3}$. In the following, we derive approximate solutions considering χ^t and χ^m as perturbations. We assume that the solutions are written as $\mathbf{r}_p(s) = a(\cos\theta,\ \sin\theta) + \Gamma(s)(\cos\theta,\ \sin\theta)$ ($\Gamma << a$). Then, Γ satisfies

$$\begin{aligned}\delta p_{eff} &+ \frac{b_1}{a^2}\Gamma + b_2\left(\frac{\Gamma_s}{a} + a\Gamma_{sss}\right) + b_3\Gamma_{ss} + b_4 a^2\Gamma_{ssss} \\ &+ 8\zeta^\circ(\chi^m\sin 2\theta - \chi^t\cos 2\theta)a^{-2} = 0, \qquad (17)\end{aligned}$$

where $\delta p_{eff} = \delta p - 3/(8\pi)P_{0\|}^2 a^{-2}\int d\theta\Gamma\cos 2\theta + 3/\pi\zeta^\circ a^{-4}\int d\theta\Gamma\cos 2\theta$, $b_1 = \Delta P\ a + 2\alpha_{\|}^\circ a^{-2} - 6\zeta^\circ a^{-2}\cos 2\theta$, $b_2 = -8\zeta^\circ a^{-2}\sin 2\theta$, $b_3 = \Delta P\ a + 4\alpha_{\|}^\circ a^{-2} - 4\zeta^\circ a^{-2}\cos 2\theta$, and $b_4 = 2\alpha_{\|}^\circ a^{-2} + 2\zeta^\circ a^{-2}\cos 2\theta$. δp is the perturbation of surface pressure to keep the domain area of perturbed solution identical to the domain area of unperturbed solution. For instance, we calculate a domain shape with weak bend orientational

deformation $\mathbf{a}_{\|}^{bend} = \mathbf{a}_x + (x/d)\mathbf{a}_y$ of the spontaneous polarization ($\nabla \cdot \mathbf{a}_{\|}^{bend} = 0$ and $\nabla \times \mathbf{a}_{\|}^{bend} = 1/d$). d represents the strength of bending deformation, and is corresponding to the distance between the center of bend deformation placed outside of a domain (0, d) and the center of a unperturbed circular domain ($d >> a$). When we express Γ by Fourier series as $\Gamma = \Sigma_n c_n \exp(in\theta)$, Eq. (17) is reduced to a recursive relation as

$$\begin{aligned}&(n^2-1)[(n-1)(n-3)c_{n-2} + (n+1)(n+3)c_{n+2} \\ &\quad + (-k_1 + k_2(n^2-1))c_n]a^{-1} \\ &\quad + k_3\delta_{n,0} - ik_4(\delta_{n,3} - \delta_{n,-3}) = 0, \end{aligned} \tag{18}$$

where $\delta_{nm} = 1$ when $n = m$, and 0 otherwise. $k_1 = \Delta P a^{-1}/(\zeta^{\circ} a^{-4})$, $k_2 = \alpha_{\|}^{\circ}/\zeta^{\circ}$ and $k_3 = \delta p_{eff} a^{-1}/(\zeta^{\circ} a^{-4})$ are the ratio of the unperturbed surface pressure, the coupling constant of $F_{\perp}$, and the perturbed surface pressure to the coupling constant of $F_{\|}$, respectively. $k_4 = 4a/d$. The recursive relation returns to that derived in ref. [19] when $k_4 = 0$. Equation (18) indicates that the odd-number-th mode and even-number-th mode of c_ns are independent. Equation (18) is identity when $n = 1$, i.e., $c_{\pm 1}$ are not determined by Eq. (18). This result is reasonable since $c_{\pm 1}$ represents translation of the domain. Equation (18) is expressed as $\mathbf{Dc} = \mathbf{g}$, where $[\mathbf{D}]_{n,n} = (n^2-1)[-k_1 + k_2(n^2-1)]$, $[\mathbf{D}]_{n,n-2} = (n^2-1)(n-1)(n-3)$, and $[\mathbf{D}]_{n,n+2} = (n^2-1)(n+1)(n+3)$, $[D]_{n,m\neq n,n\pm 2} = 0$, $[c]_n = c_n$, $[g]_{n=\pm 3} = \pm ik_4$, $[\mathbf{g}]_0 = -k_3$, and $[\mathbf{g}]_{n\neq \pm 3,0} = 0$ ($n \leq -3$ or $3 \leq n$). Here, $[\mathbf{A}]_{m,n}$ is the *(m, n)* component of matrix $\mathbf{A}$. When $det\mathbf{D} \neq 0$, the solution is expressed as $c_{2m}/a = -[\mathbf{D}^{-1}]_{2m,0}k_3$, $c_{2m+1}/a = i[\mathbf{D}^{-1}]_{2m+1,3}k_4\,(m > 0)$, and $c_{2m-1}/a = -i[\mathbf{D}^{-1}]_{2m-1,-3}k_4\,(m < 0)$. $k_3(\propto \delta p_{eff})$ is determined by the constraint of constant area $c_0/a = -1/2\sum_n |c_n|^2/a^2$ as $k_3^{(1)} \sim 1/2\sum_m [D^{-1}]_{2m+1,\pm 3}^2/[D^{-1}]_{0,0}k_4^2$ and $k_3^{(2)} \sim [D^{-1}]_{0,0}/(1/2\sum_m [D^{-1}]_{2m,0}^2)$. However, it is not reasonable to consider that $k_3^{(2)}$ is a solution since $k_3^{(2)}$ does not depend on the perturbation k_4. Thus, k_3 and c_{2m}s are proportional to k_4^2, and can be neglected in our first order perturbation analysis.

It is not difficult to calculate $\mathbf{D}^{-1}$ numerically when k_2 is large ($k_2 > 2.5$), i.e., the coupling constant of $F_{\|}$ is smaller than that of $F_{\perp}$. In our present study, we take into account only the odd-number-th components of $\mathbf{D}^{-1}$ since even-number-th components are neglected as we have already discussed. The domain shape with $k_1 = 12.5$, $k_2 = 2.5$, and $k_4 = 0.3$ is shown in Figure 4(a), where it is corresponding to a monolayer domain with e.g. $a = 10\,\mu\text{m}$, $d = 134\,\mu\text{m}$, $P_{0\perp} = 4.23 \times 10^{-2}\,\text{C/m}$, $P_{0\|} = 3.00 \times 10^{-2}\,\text{C/m}$, and $\Delta P = 0.28\,\text{mN/m}$. These values are chosen based on our experimental study using MDC-SHG measurement on phospholipid monolayers [5,24]. Γ/a and $\sigma_{induced}/P_{0\|}$

of domains with shape perturbation are plotted by the solid curves in Figures 4(b) and (c), respectively. The dashed curves in Figures 4(b) and (c) represent Γ/a and $\sigma_{induced}/P_{0\|}$ of domains without shape perturbation in the presence of bend orientational deformation ($\Gamma/a = 0$). Figure 4(a) indicates that domains with bend orientational deformation form egg-like shape at the state ($k_1 = 12.5$, $k_2 = 2.5$, and $k_4 = 0.3$). Similar shapes have been observed from DMPA monolayer domains ($a \sim 20\,\mu\text{m}$) by Kjaer *et al.* [23]. As k_4 increases, the calculated domain shapes become closer to the observed shapes. The solid and dashed curves in Figure 4(c) is the charge density distribution of domains with and without taking into account the contribution of the shape perturbation Γ/a from circular domain, respectively, in the presence of bend orientational deformation. In region (v), positive and negative charges of solid curve at $\theta > z_2$ and $\theta < z_2$, respectively, are larger than the dashed curve at the vicinity of z_2, where $\sigma_{\text{induced}}/P_{0\|} = 0$ (see Fig. 4(c)). The positive and negative peaks of solid curve in region (iv) and (vi) are smaller than the corresponding peaks of dashed curve. The attractive interaction is strong at the vicinity of z_2, where the polarity of the induced charges changes, whereas repulsive interaction is strong at the positions, where the induced charge of the same polarity is large (see Fig. 4(c)). The shape perturbation changes the distribution of induced charge density at the domain boundary so that the attractive interaction in region (v) increases and the repulsive interaction in region (iv) and (vi) decreases, i.e. the total free energy of the domain decreases. Thus, our present result is reasonable from the viewpoint of electrostatic charge effect. However, the shape perturbation in region (i)–(iii) is not determined in the same way. It is possibly because the line tension makes a more important contribution than electrostatic energy in region (i)–(iii). On account of bend orientational deformation, electrostatic charge density increases in region (iv)–(vi), and decreases in region (i)–(iii) (see the dashed curve of Fig. 4(c)). In other words, the bend orientational deformation makes the contribution of electrostatic energy weaker, and the line tension rather makes an important contribution in region (i)–(iii). For this reason, the shape perturbation in region (iv)–(vi) is induced by the electrostatic charge effect whereas the additional generation of shape perturbation is suppressed by the line tension in region (i)–(iii) (see Fig. 4(c)). In this analysis, it is exemplified that the orientational deformation determines the significance of the contribution of electrostatic energy $F_{\|}$ due to the generation of in-plane spontaneous polarization to the formation of domain shapes, and the domain shapes with induced charge density distribution at the domain boundary, which optimizes the electrostatic energy, Eq. (6).

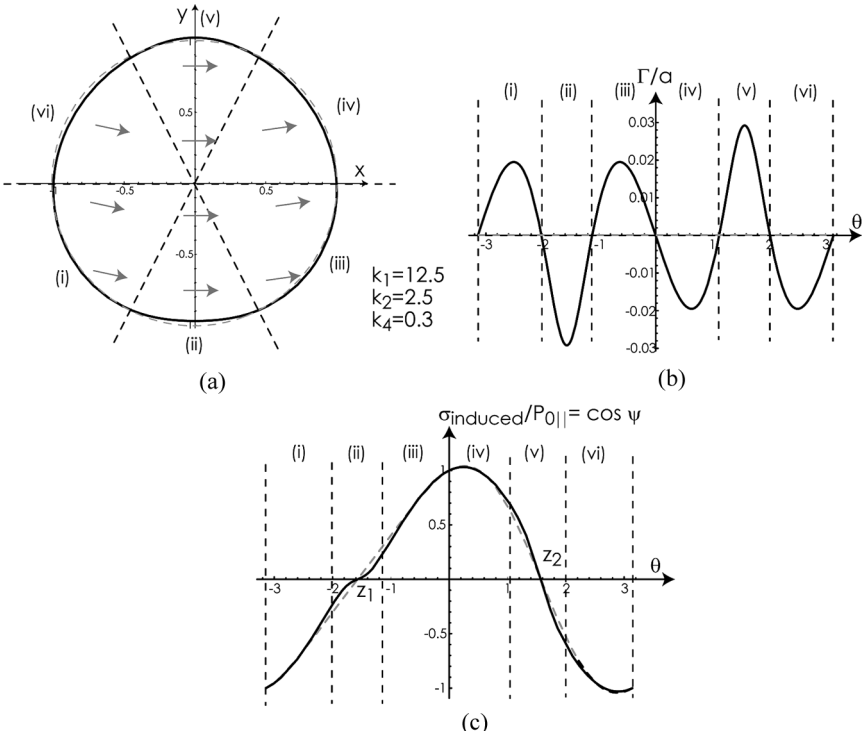

FIGURE 4 A shape of domain with bend orientational deformation of spontaneous polarization obtained by Eq. (18) for $k_1 = 12.5$, $k_2 = 2.5$, and $k_4 = 0.3$ (the black solid curve of (a)). The center of bend deformation is placed at (0, d) in the (x, y) coordinate shown in (a). The gray dashed curve is the unperturbed solution (circle). The orientation of spontaneous polarization is schematically drawn by the gray arrows. Γ/a and $\sigma_{induced}/P_{0||}$ of this domain shape is plotted to (b) and (c). The regions (i)–(vi) of (b) and (c) are consistent with (a). $\sigma_{induced}/P_{0||}$ without the contribution of Γ/a is also plotted to the dashed curve in (c). $\Gamma/a = 0.0217 \sin 3\theta - 0.0052 \sin 5\theta + 0.00155 \sin 7\theta - 0.00051 \sin 9\theta + 0.00018 \sin 11\theta - 0.000068 \sin 13\theta$.

The latter effect is nothing but the spontaneous curvature. In other words, the effect of the spontaneous curvature is successfully incorporated in the shape equation (16).

IV. CONCLUSION

The forming mechanism of monolayer domain shapes with orientational deformation is investigated from the viewpoint of differential

geometry. The curvature of polarization is introduced to represent the orientational deformation, and the shape equation is extended taking into account the contribution of spontaneous curvature. As a model calculation, we derived an approximate solution of domains with bend orientation. It is exemplified that the spontaneous curvature is reasonably understood as shape formation to optimize the off-diagonal component of electrostatic energy. In the review process of this article, we made a progress on taking into account the contribution of Frank elastic energy and spontaneous splay (Eq. (8) and (9)) in the shape equation for the further understanding on the forming mechanism of monolayer domain shapes and discussed in Ref. [25] in details.

REFERENCES

[1] Gaines, G. L. (1966). *Insoluble Monolayers at Liquid-Gas Interfaces*, Interscience: New York.
[2] Kaganer, V. M., Mohwald, H., & Dutta, P. (1999). *Rev. Mod. Phys.*, *71*, 779.
[3] de Gennes, P. G. & Prost, J. (1995). *The Physics of Liquid Crystals*, Clarendon Press: Oxford.
[4] Iwamoto, M. & Wu, C. X. (2000). *The Physical Properties of Organic Monolayers*, World Scientific: Singapore.
[5] Tojima, A., Manaka, T., & Iwamoto, M. (2001). *J. Chem. Phys.*, *115*, 9010.
[6] Iwamoto, M., Tojima, A., Manaka, T., & Ou-Yang, Z. C. (2003). *Phys. Rev. E*, *67*, 041711.
[7] Iwamoto, M. & Ou-Yang, Z. C. (2005). *Phys. Rev. E*, *72*, 021704.
[8] Yamamoto, T., Taguchi, D., Manaka, T., & Iwamoto, M. (2005). *J. Chem. Phys.*, *122*, 164703.
[9] Wagner, R., Yamamoto, T., Manaka, T., & Iwamoto, M. (2005). *Rev. Sci. Instrum.*, *76*, 083902.
[10] Wagner, R., Yamamoto, T., Manaka, T., & Iwamoto, M. (2006). *Colloids and Surfaces A : Physicochem. Eng. Aspects*, *284–285*, 147.
[11] Henón, S. & Meunier, J. (1991). *Rev. Sci. Instrum.*, *62*, 936.
[12] Honig, D. & Möbius, D. (1991). *J. Chem. Phys.*, *95*, 4590.
[13] Schwartz, D. K., Tsao, M. W., & Knobler, C. M. (1994). *J. Chem. Phys.*, *101*, 8258.
[14] Weidemann, G. & Vollhardt, D. (1995). *Colloids and Surfaces A : Physicochem. Eng. Aspects*, *100*, 187.
[15] Moy, V. T., Keller, D. J., & McConnell, H. M. (1988). *J. Phys. Chem.*, *92*, 5233.
[16] McConnell, H. M. & Moy, V. T. (1988). *J. Phys. Chem.*, *92*, 4520.
[17] Lee, K. Y. C. & McConnell, H. M. (1993). *J. Phys. Chem.*, *97*, 9532.
[18] Iwamoto, M. & Ou-Yang, Z. C. (2004). *Phys. Rev. Letts.*, *93*, 206101.
[19] Iwamoto, M., Liu, F., & Ou-Yang, Z. C. (2006). *J. Chem. Phys., 125*, 224701.
[20] Ou-Yang, Z. C., Xing, L. J., & Zhang, X. Y. (1999). *Geometrical Methods in the Elastic Theory of Membranes in Liquid Crystal Phases*, World Scientific: Singapore.
[21] Rudnick, J. & Bruinsma, R. (1995). *Phys. Rev. Letts.*, *74*, 2491.
[22] Yamamoto, T., Manaka, T., & Iwamoto, M. *Thin Solid Films*, (accepted).
[23] Kjaer, K., Als-Nielsen, J., Helm, C. A., Laxhuber L. A., & Möhwald, H. (1987). *Phys. Rev. Letts.*, *58*, 2224.
[24] Iwamoto, M., Kubota, T., & Ou-Yang, Z. C. (1996). *J. Chem. Phys.*, *104*, 736.
[25] Yamamoto, T., Manaka, T., & Iwamoto, M. *J. Chem. Phys.*, (submitted).